High Pressure Preparation and Properties of Polycrystalline Oxides and Halides

A.J. DeLai, R.M. Haag, and J.K. Hill

AVCO CORPORATION
Research and Advanced Development Division
Wilmington, Massachusetts 01887

The high pressure research studies conducted in this laboratory have been of three types. Microstructure and physical properties of dense oxides prepared at high pressure and relatively low temperature have been studied. Among the compounds investigated have been alumina, magnesia, and chromia.

In other studies the preparation of "new" materials by "irreversible" transformations at high pressure was undertaken. By this we mean the metastable retention at atmospheric pressure of materials or phases thermodynamically stable only at higher pressure.

Physical measurements, specifically compressibility measurements at high pressure are being undertaken.

We have designed and constructed two belt-type cells. The first offers a sample volume, within the gasket, 0.500 inches in diameter and 1 inch in length. A pressure of one million psi or approximately 70 kilobars can be achieved with this apparatus. The second with a sample diameter of 0.125 inches and the same length is capable of achieving three million psi or approximately 200 kilobars. With resistive heating, temperatures to 1500°C can be obtained in either of these systems. This apparatus consists essentially of a belt type die body with a carbide insert and carbide punches. A 400--ton press is used for operation. The assembly is shown in Figure 1.

At high pressures (greater than 30 kilobars) nearly complete densification of oxide powders is achieved at much lower temperature and in shorter time than is otherwise required. Under these conditions, dense material with a very fine grain size is obtained. A good example of the microstructure studies is afforded by our investigations of the properties of MgO formed at high pressures. Electronic grade MgO with an initial particle size of 300 Å (from x-ray line broadening measurements) or 500 Å (from electron microscopic examination) was densified at pressures of 12.5 kilobars and above and temperatures between 500 and 1000°C. At 12.5 kilobars and 900°C, essentially complete densification was achieved in 5 to 10 minutes. The material was transparent in 1/16 inch sections. Electron micrographic examination showed a grain size in the submicron range (approximately ~~0.5~~ 0.05 micron, 500 angstroms) as shown in Figure 2. X-ray diffraction line broadening showed an apparent grain size of about 500 Å indicating considerably strain. The Knoop hardness of this material was about 1200 Kg/mm^2 under a 100 gram load as compared with 600 for single crystal MgO and 800-900 Kg/mm^2 for hot pressed MgO.

Although the development of improved properties by ultrahigh pressure forming could be discussed at more length, I want to go on to other studies at this time.

The rare earths, that is the sesquioxides, are found in three distinct structural forms. The first of these is the hexagonal or A-R_2O_3 structure which is typified by La_2O_3. The second is the monoclinic or B-R_2O_3 structure and the third is the cubic or C-R_2O_3 structure which is the same as that of Mn_2O_3. In general, the rare earth metal ions with the largest radii; e.g., lanthanum, form the hexagonal oxide, and those with the smallest radii form the cubic oxide. Many of the rare earths can be obtained in two modifications. Thus, samarium oxide is found in both the cubic - C and monoclinic - B forms.

Investigations of the stability limits of the various structural modifications have been carried out for a number of years. The range of stability of the three modifications as a function of cation-radius and temperature as proposed by Shafer and Roy is shown in Figure 3. It is evident from this figure that samarium oxide lies near the border between the A - and B - type fields at high temperature. However, the A-type oxide of samarium has not been observed either in high-temperature x-ray studies nor in room-temperature examination of material quenched from high temperatures.

In the hexagonal oxide each cation has seven nearest oxygen neighbors compared with six such neighbors in the other structures. This results in a greater density in the hexagonal modification compared with the other two forms. Thus, in the case of neodymium oxide, the relative volumes are A:B:C = 75.5:77.7:84.6 ($A^{\circ 3}$/FW). It seemed that if the A-modification of Sm_2O_3 could be formed that both high temperature and high pressure would be required. Accordingly, we have examined material quenched from high temperature at pressures to 30 kilobars. In no case was any trace of an hexagonal modification observed.

Experimentally, C-form (cubic) oxide (d = 10.89 Å) obtained from Research Chemicals Corporation was prepressed in a steel die to approximately 50% of theoretical density. This compact was loaded into a nickel tube and into the high pressure apparatus described previously. Some samples were instrumented with thermocouples, others were not. In the absence of such instrumentation the temperature of the run was estimated from the power settings as calibrated in the instrumented runs.

In eight runs at 30 kilobars and temperatures between 575°C and 925°C the C-form was converted to the more dense B-form. At the lowest temperature the

conversion was incomplete. In two runs, one at 580° and one at 925° the monoclinic form was used as the starting material. No conversion of this oxide was observed.

X-ray diffraction analysis of the products of the high pressure runs revealed, in addition to the two oxides, various hydroxides and oxyhydroxides. The water for the formation of these compounds comes from the decomposition at elevated temperature of the pyrophyllite gasket material. We have observed both of the previously reported hydroxides and the previously reported oxyhydroxide SmOOH. In addition, we have found a new phase which we call β-SmOOH.

Weight loss versus temperature curves from preparations showing only the x-ray diffraction lines of the new phase were obtained. These are shown in Figure 4. In each case the sample was heated in air for one hour at the indicated temperature, cooled, weighed and reheated to the next higher temperature. The weight loss begins above 300°C and constant weight is observed above 700°C. In one case a small aliquot was taken for x-ray diffraction analysis after heating to 500°C. The curve shows this as a weight loss. The curve has not been renormalized for this loss since the displacement of the curve is small. Shown in the same figure is Sm_2O_3-H_2O. In a separate experiment a sample was heated in vacuum to 700°C. The evolved gases were condensible at the temperature of liquid nitrogen and the weight loss was comparable to that reported above. Therefore, it is assumed that the new phase has the composition SmOOH.

Infrared measurements were made with a Perkin Elmer Model 221 spectrometer. The sample was scanned in the wavelength range from 2.5 to 16 microns using both KBr pellet and petrolatum mull techniques. The OH stretching vibration at 2.93 micron was observed together with the bending vibration at 6.8 microns. In addition, unassigned absorption peaks between 11 and 15 microns were observed.

Beta-SmOOH is light yellow in color. Since no single crystals could be isolated, optical properties could not be determined. It was, however, determined to be optically anisotropic with an average index of refraction of approximately 1.93.

The x-ray diffraction results are shown in Figure 5. These have been indexed on a tetragonal unit cell with $a_o = 8.07$, $c_o = 11.2$. The observed density, 6.62 grams per cc, gives 15.9 formula weights per unit cell. This is reasonable for a tetragonal structure. We assume therefore 16 formula units per unit cell and a theoretical density of 6.66. As indicated above no single crystals could be isolated and no more detailed studies could be performed.

However, it should be noted that by a 45° rotation around the C-axis, a nearly cubic cell can be obtained with sides averaging about 11.3 Å which contains 32 formula units, that is $H_{32}Sm_{32}O_{64}$. This cube is only slightly larger than that of the defect fluorite lattice of cubic Sm_2O_3 and contains just enough excess oxygen ions to fill the vacancies in that structure. In fact a fair fit of the stronger lines to a cube with $a_o \sim 5.70$ expedited the determination of the tetragonal unit cell given above. It is reasonable then to postulate a structure based on the fluorite structure and to ascribe the shortening of the C-axis, relative to the A-axis to hydrogen bonding.

Beta-SmOOH is easily converted to the hydroxide by boiling in water for fifteen minutes. After air drying at 110°C, the weight loss on ignition to 1100°C is 12.6%, corresponding to the loss of 1.49 moles of H_2O per mole of starting SmOOH. X-ray diffraction examination of this hydroxide gave the results shown in Figure 6. These d-values have not been indexed and do not correspond to either of the two reported hydroxides as shown in the same table. Note that

this hydroxide is not the same as the high pressure modification prepared by Shafer and Roy. It is derived from a high-pressure modification of SmOOH.

In addition to these studies, high pressure x-ray diffraction studies have been performed with a camera similar to that described by Mariano. In this camera, high pressure is achieved between diamond anvils. A collimated beam is brought through one diamond. The diffracted rays pass out through the other diamond and impinge on a flat photographic plate or film.

With powder specimens, Debye rings are formed and the interplanar spacings d may be calculated from the formula

$$d = \frac{\lambda}{\sqrt{2}\left[1 - (1/1 + x^2)^{1/2}\right]^{1/2}}$$

where λ is the wavelength of the radiation employed and x is the ratio of the measured radius of the Debye ring to the sample-to-film distance.

The compressibility β_T is defined as $-1/V\ (\partial V/\partial P)_T$ but this is just three times the linear dilatation $1/d\ (\partial d/\partial P)$. Differentiating the expression above with respect to pressure, we can obtain

$$\beta = \frac{3X \quad \partial X/\partial P}{2\ (1 + x^2)\ \left[(1 + x^2)^{1/2} - 1\right]}$$

or for finite changes

$$\beta = \frac{3X \quad \Delta X/\Delta P}{2\ (1 + x^2)\ \left[(1 + x^2)^{1/2} - 1\right]}$$

In order to measure the compressibility then, we measure the line shift observed between exposures at different pressures. By superimposing exposures at different pressures on the same film, errors due to changes in sample-to-film distance, or film shrinkage, etc. are avoided. The line displacement which is proportional to the compressibility is easily estimated visually to one twentieth of a millimeter. Attempts have been made to resolve the shifted lines with a densitometer in order to achieve even greater precision. However, at convenient exposure levels this could not be done.

Extrusion of the sample from between the faces of the diamond anvils results in a loss in intensity of the diffraction rings and, if extensive, in a reduction in pressure under the anvils by filling the space around the anvils, and absorbing some of the load. Powder samples have been prepared in several ways to avoid this difficulty. The best samples have been prepared by prepressing at about 1000 psi either dry powders or powders which have been infiltrated with parlodion.

Before pressing, a copper specimen support 2 1/2 mm in diameter with a 0.8 mm central hole is placed on the powder. During pressing the powder is forced into this hole. The excess powder is trimmed away and the sample is mounted between the diamond anvils. This copper ring gives lateral support to the sample.

Typical photographs are shown in Figures 7 and 8. The sample material is rubidium chloride. The first figure shows two exposures at ~25 kilobars and at 1 atm. Lines are observed of both the high pressure form with the cesium chloride structure and the low pressure from with the rock salt structure. Also visible are Laue' spots from the two diamond crystals.

The next figure shows two exposures at 40 kilobars and 60 kilobars. In this case, only the high pressure form is present. The splitting of the (110) and (200) lines can be seen, the latter more clearly than the former. Using the known compressibility of the low pressure form to calibrate the cell, the compressibility of the high pressure form above the transition pressure is 5.6×10^{-3} $Kbar^{-1}$.

In closing, we want to acknowledge the support and encouragement given to this work by the Office of Aerospace Research, United States Air Force, AFCRL and particularly to Dr. Johannes Plendl, Dr. Peter Gielisse and Mr. Larry Mansur.

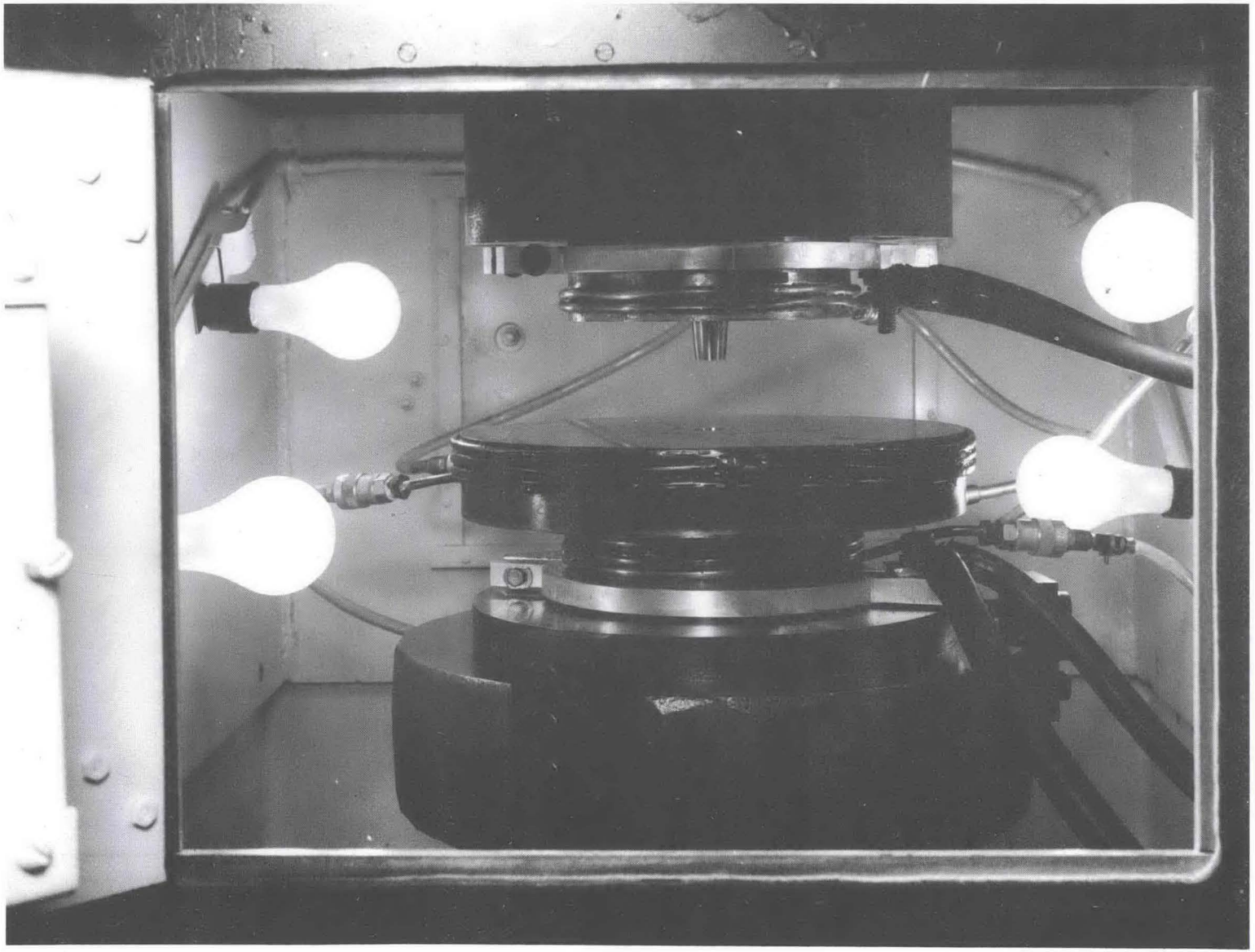

High Pressure Apparatus

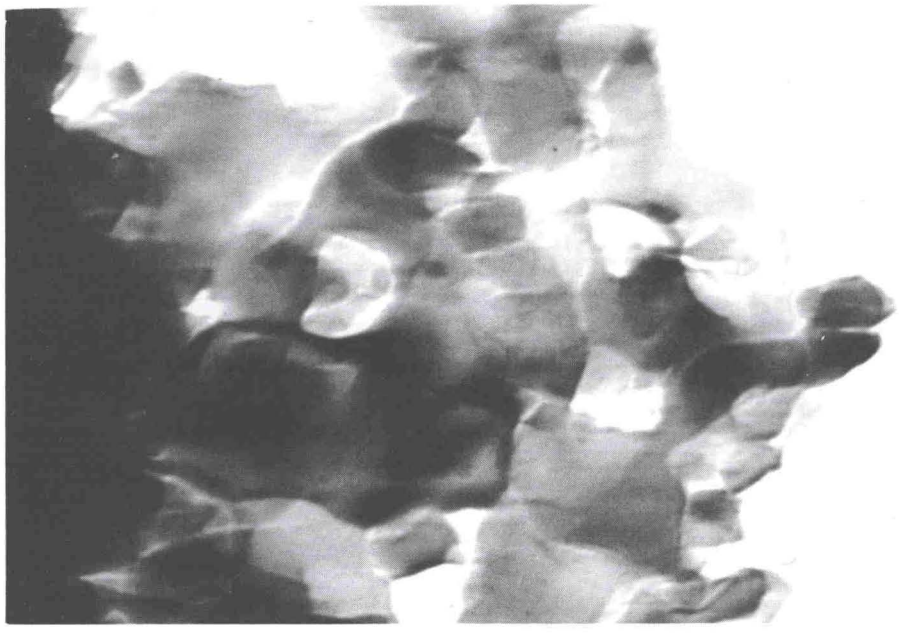

#640053 240,000X

Figure 2 Transmission Electron Micrograph of MgO
Grain Size 500 Å

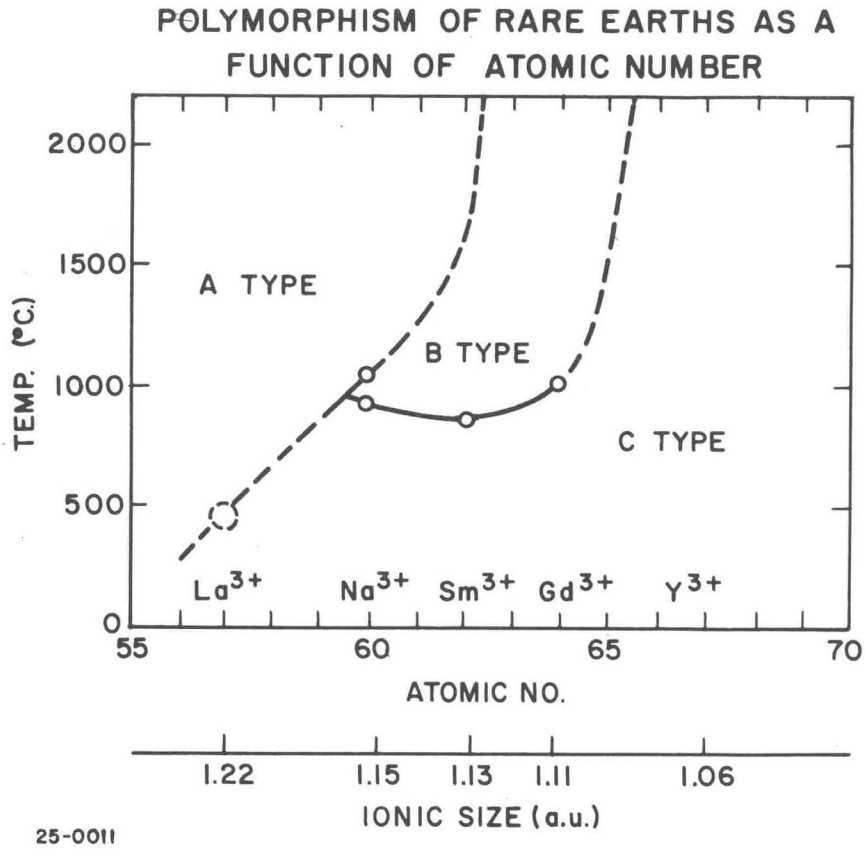

Figure 3 Polymorphism of Rare Earths as a Function of Atomic Number

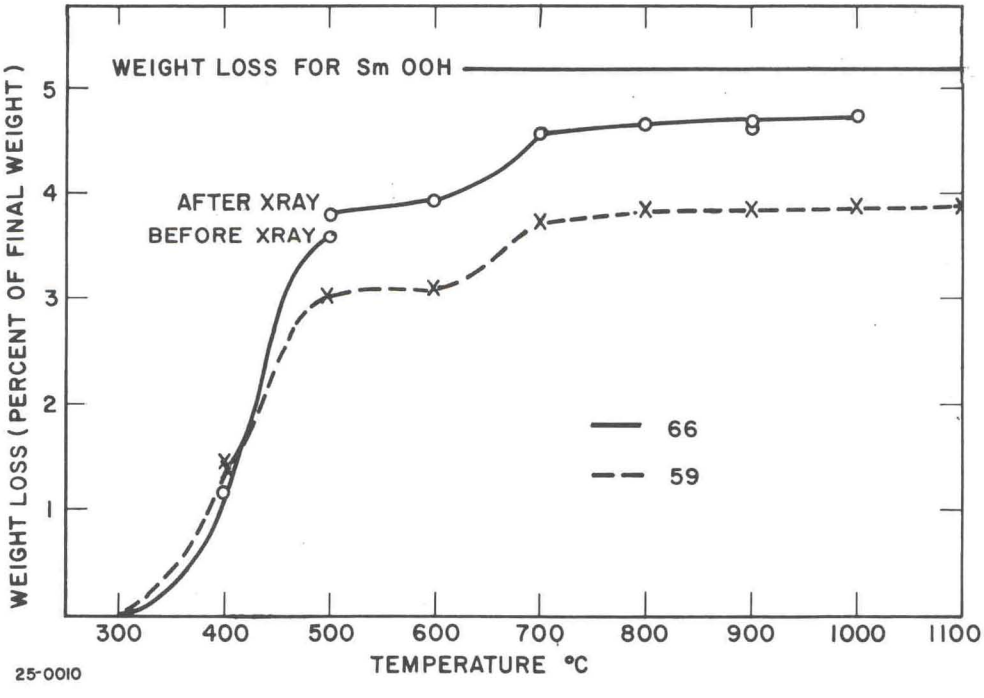

Figure 4 Weight loss versus temperature for SmOOH

X-RAY DIFFRACTION RESULTS β - SmOOH

d	I/I_1	hkl
5.609	10	(002)
5.068	3	(111)
4.004	9	(112)
3.290	100	(202)
2.867	50	(220)
2.814	15	(004)
2.557	10	(310)(222)
2.309	25	(204)
2.023	22	(400)
2.002	30	(224)(401)
1.892	9	(314)(331)
1.804	12	(332)(420)
1.722	28	(305)(422)
1.698	12	(206)(333)
1.639	7	(404)(423)
1.563	12	3 LINES
1.519	10	(424)

25-0013

Figure 5 X-ray Diffraction Results of B-SmOOH

COMPARISON OF X-RAY RESULTS $Sm(OH)_3$

$Sm(OH)_3$ this work		$Sm(OH)_3$ Hexagonal			$Sm(OH)_3$ High Pressure Form	
d	I/I	d	I/I	hkl	d	I/I
5.609	80	5.54	100	(100)	7.816	25
3.296	5	3.16	70	(110)	5.566	35
3.251	60	3.03	55	(101)	3.723	80
3.084	100	2.734	15	(200)	3.363	5
2.780	20	2.183	90	(201)	3.089	40
2.423	8	2.064	15	(210)	2.852	5
2.222	70	1.821	50	(300)	2.768	25
2.099	15	1.795	65	(211)	2.583	100
1.848	35	1.575	15	(220)	2.089	30
1.824	55	1.519	7	(310)	2.057	5
1.751	8	1.400	20	(311)	1.843	45
1.599	25	1.366	10	(400)	1.819	5
1.537	6	1.284	10	(401)	1.596	15
1.415	13	1.194	10	(410)	1.592	10
1.384	6				1.548	20
1.307	8				1.534	10
					1.382	5
					1.290	10
					1.206	10
					1.204	5

25-0012

Figure 6 Comparison of X-Ray Results of $Sm(OH)_3$

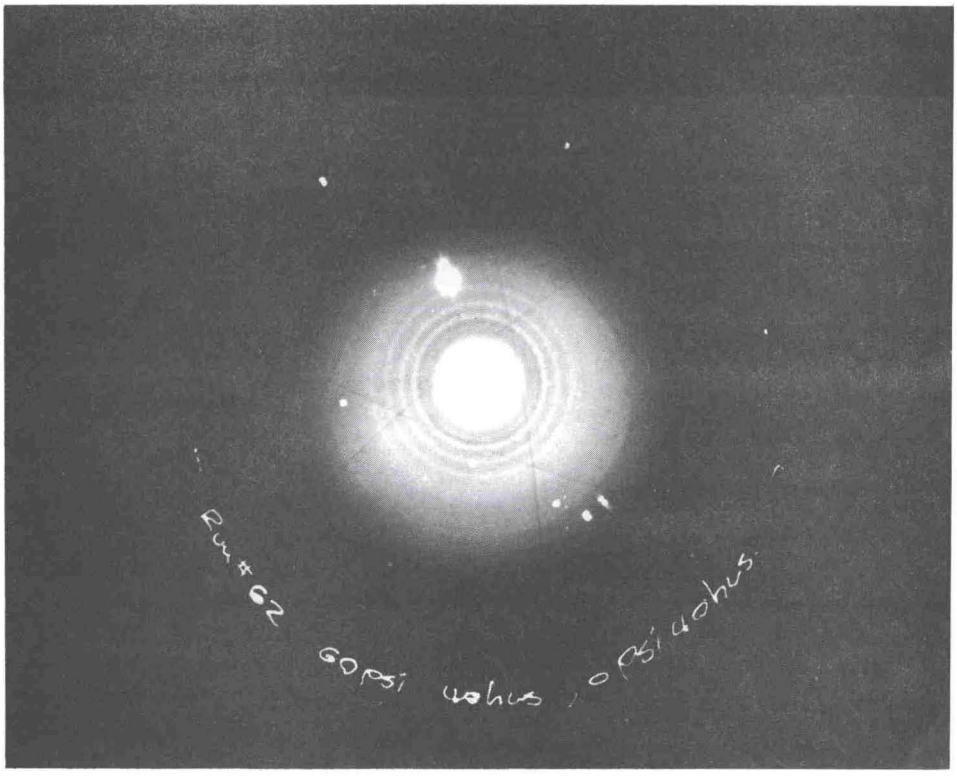

Figure 7 X-Ray Patterns of RbCl at 1 bar and at 25 kilobars

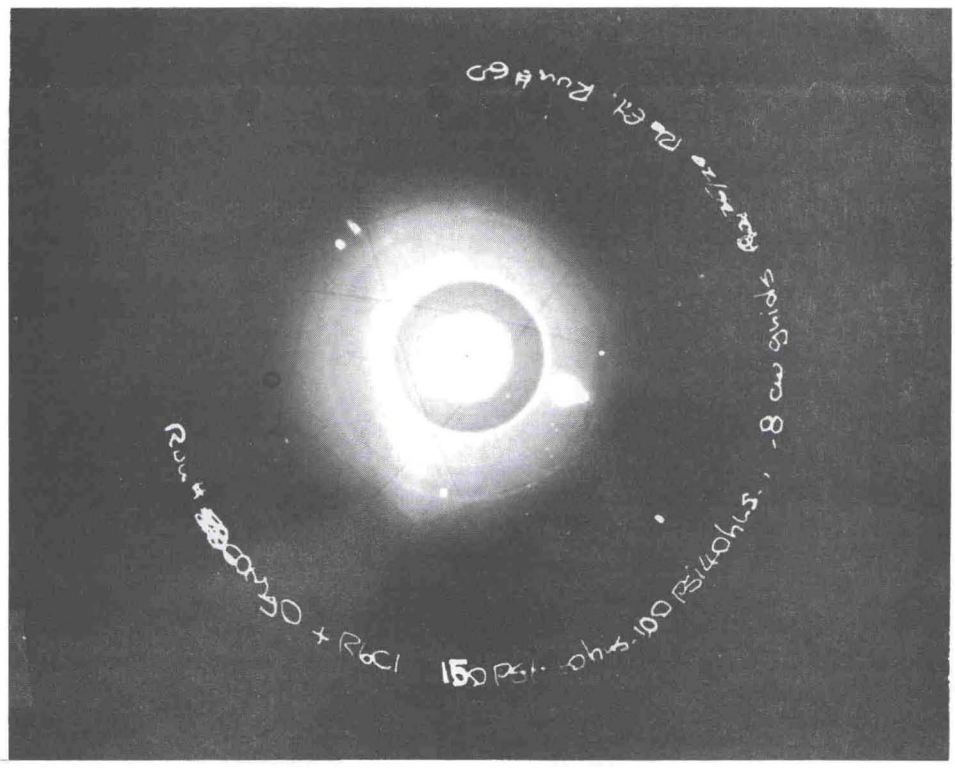

Figure 8 X-Ray Patterns of RbCl at 40 and 60 kilobars